Nuclear Engineering and Design 300 (2016) 506–516

Contents lists available at ScienceDirect

Nuclear Engineering and Design

journal homepage: www.elsevier.com/locate/nucengdes

Development, validation and application of multi-point kinetics model in RELAP5 for analysis of asymmetric nuclear transients

Santosh K. Pradhan[a,*], K. Obaidurrahman[a], Kannan N. Iyer[b], Avinash J. Gaikwad[a]

[a] Nuclear Safety Analysis Division, Atomic Energy Regulatory Board, Mumbai 400094, India
[b] Department of Mechanical Engineering, IIT Bombay, Mumbai 400076, India

HIGHLIGHTS

- A multi-point kinetics model is developed for RELAP5 system thermal hydraulics code.
- Model is validated against extensive 3D kinetics code.
- RELAP5 multi-point kinetics formulation is used to investigate critical break for LOCA in PHWR.

ARTICLE INFO

Article history:
Received 30 September 2015
Received in revised form
25 December 2015
Accepted 30 January 2016
Available online 8 March 2016

D. Reactor engineering

ABSTRACT

Point kinetics approach in system code RELAP5 limits its use for many of the reactivity induced transients, which involve asymmetric core behaviour. Development of fully coupled 3D core kinetics code with system thermal-hydraulics is the ultimate requirement in this regard; however coupling and validation of 3D kinetics module with system code is cumbersome and it also requires access to source code. An intermediate approach with multi-point kinetics is appropriate and relatively easy to implement for analysis of several asymmetric transients for large cores. Multi-point kinetics formulation is based on dividing the entire core into several regions and solving ODEs describing kinetics in each region. These regions are interconnected by spatial coupling coefficients which are estimated from diffusion theory approximation. This model offers an advantage that associated ordinary differential equations (ODEs) governing multi-point kinetics formulation can be solved using numerical methods to the desired level of accuracy and thus allows formulation based on user defined control variables, i.e., without disturbing the source code and hence also avoiding associated coupling issues. Euler's method has been used in the present formulation to solve several coupled ODEs internally at each time step. The results have been verified against inbuilt point-kinetics models of RELAP5 and validated against 3D kinetics code TRIKIN. The model was used to identify the critical break in RIH of a typical large PHWR core. The neutronic asymmetry produced in the core due to the system induced transient was effectively handled by the multi-point kinetics model overcoming the limitation of in-built point kinetics model of RELAP5 and standalone 3D core kinetics codes.

© 2016 Elsevier B.V. All rights reserved.

1. Introduction

Assessment of the safety of an NPP requires that behaviour of the plant following a Postulated Initiated Event (PIE) be analyzed. Also, the plant, its' systems and equipment should be designed to ensure that under normal operation, during operational transients and accident conditions, acceptance criteria are not exceeded. One of the most important PIEs for design of Pressurized Heavy Water Reactor (PHWR) based Nuclear Power Plants (NPP) is the Loss of Coolant Accident (LOCA). For a particular range of breaks in Reactor Inlet Header (RIH), gross flow stagnation may occur in coolant channels in the reactor core leading to rise in fuel temperature. The size of the break that leads to maximum rise in clad surface temperature is called critical break. The critical break in RIH imposes most stringent requirement on Emergency Core Cooling System (ECCS) as the clad surface temperature reaches maximum. Class IV power supply is the main power output supply and it is directly connected to main grid power supply and main plant

Abbreviations: ASDV, atmospheric steam dump valve; ECCS, emergency core cooling system; IRV, instrumented relief valve; IQS, improved quasi-static; LOCA, loss of coolant accident; LORA, loss of regulation accident; LWR, light water reactor; NPP, nuclear power plant; PCP, primary circulating pump; PCT, peak clad temperature; PHT, primary heat transport; PHWR, pressurized heavy water reactor; PIE, postulated initiated event; RIH, reactor inlet header; ROH, reactor outlet header; SG, steam generator; SRV, safety relief valve; TDV, time dependent volume.

* Corresponding author. Tel.: +91 22 25990466; fax: +91 2225990499.
E-mail address: santosh@aerb.gov.in (S.K. Pradhan).

http://dx.doi.org/10.1016/j.nucengdes.2016.01.028
0029-5493/© 2016 Elsevier B.V. All rights reserved.

Nomenclature

$\emptyset$	neutron flux
Σ_a	macroscopic absorption cross section
Σ_{12}	macroscopic scattering cross section (from fast to thermal)
Σ_{21}	macroscopic scattering cross section (from thermal to fast)
β	effective delayed neutron fraction
ν	number of neutrons produced per fission
Σ_f	macroscopic fission cross section
λ_i	decay constant of ith delayed neutron group
β_i	delayed neutron fraction of ith group
ρ	reactivity
α	coupling coefficient
v	neutron velocity
t	time
D	diffusion coefficient
$\tilde{C}_i$	precursor concentration of ith delayed neutron group
J	neutron current density
A	interface area between nodes
V	volume of a node
P	power of a node
C_i	delayed neutron concentration of ith group expressed in terms of power
Z	number of nodes
m_d	number of delayed neutron groups
l	prompt neutron life time
K	infinite multiplication factor
∇	del operator
Δ	distance between nodes

generator. Class-IV power supply is derived from grid through start-up transformer and from the turbo-generator system through generator transformer and unit transformer. The loads connected to this system can tolerate prolonged power supply interruption. The size of critical break at RIH will also depend on whether class-IV power supply is available or not. In the present paper, the analysis to identify the critical break in RIH with class-IV power supply unavailable in a typical large PHWR is presented.

The considered PHWR consists of two figure of eight loops and the postulated break occurs in one RIH of one loop leading to neutronically asymmetric behaviour. Considering the core characteristic size (dimensions expressed in terms of neutron migration length) beyond 30, the core is categorized as neutronically loosely coupled (Obaidurrahman and Singh, 2010). As the reactor is loosely coupled, the development and use of multi-point kinetics model to analyse the unsymmetrical core behaviour event mentioned above is required. In the present development, the in-built point kinetics model of RELAP5 was put off and user defined multi-point kinetics models were introduced. The neutron balance equation along with concentration of delayed neutron pre-cursor was solved using Euler's method for every time step. The calculated power was fed into the fuel bundles modelled as heat structures. Diffusion of neutron from one core region to the other was accounted through coupling coefficients in multi-point kinetics equations. The results were verified against inbuilt point-kinetics model of RELAP5 and validated against in-house 3D kinetics code TRIKIN. A range of break sizes ranging from 5% to 100% of double ended guillotine rupture of RIH were analysed using this multi-point kinetics model and the critical break was identified.

Though multi-point kinetics approach is in use for control studies involving core asymmetry (Shimjith et al., 2010), it has not been incorporated with system thermal hydraulic codes to analyse neutronic asymmetric transients generated due to asymmetric thermal hydraulic behaviour or feedback. In this paper an innovative approach is adopted to develop multi-point kinetics coupled with system thermal hydraulics code and apply the same to analyse a neutronic asymmetry transient with thermal hydraulics feedbacks.

2. Point kinetics model of RELAP5

The best estimate system thermal hydraulics code RELAP5/MOD3.4 has been developed by the Idaho National Engineering Laboratory and being extensively used for analysing postulated accidents and transients in water cooled reactor systems. The detailed description of code structure, system models and correlations, solution methods, user guidelines, input requirements, etc. are provided in different volumes of RELAP5/Mod 3.4 Code Manuals (Information Systems Laboratories Inc, 2001). The principal feature of the RELAP5/MOD3.4 is the use of a two-fluid, non-equilibrium and non-homogeneous hydrodynamic model for transient simulation of the two-phase system behaviour. The field equations are coupled by point kinetics model to permit simulation of feedback between neutronics and thermal hydraulics. The point kinetics ODEs are solved using the modified Runge–Kutta method of Cohen and are advanced with the same time step as the thermal fluids and heat conduction equations, and reactivity is assumed to vary linearly between time step values. The data exchange between the point kinetics calculation and the other calculations are explicit. The point kinetics calculations lag the thermal fluids, heat conduction and heat transfer calculations. The reactor power used in thermal fluids and heat conduction is the value at the beginning of the time step. The end of time step values from thermal fluids and heat conduction calculations are used to compute the reactivity used in the point kinetics calculations. A schematic of the data exchange between reactor

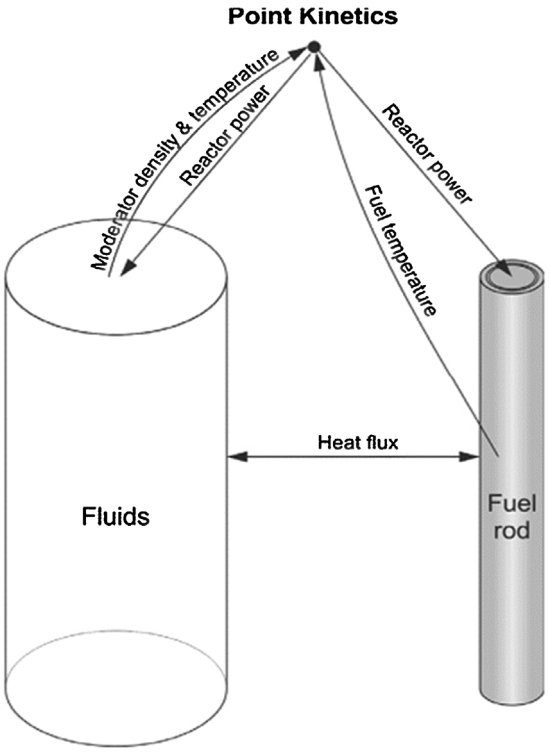

Fig. 1. Schematic of data exchange in RELAP5 in coupled point kinetics calculations (Zhang et al., 2013).

kinetics and thermal-hydraulics is shown in Fig. 1 (Zhang et al., 2013). Coupled point kinetics with system thermal hydraulics calculations are widely used for safety analysis of LWRs and PHWRs (Espinosa-Paredes and Nunez-Carrera, 2008; Pradhan et al., 2012).

Point kinetics approach in the system code RELAP5 limits its use for many reactivity induced transients, which involve asymmetric core behaviour. To circumvent this inadequacy, multi-point kinetics method was developed and implemented. Development of full 3D core kinetics code is ultimate requirement in this direction; however coupling and validation of 3D kinetics module with system code requires access to source code and is resource intensive. An intermediate approach of multi-point kinetics is appropriate and relatively easy to implement for analysis of several asymmetric transients in the large cores.

3. Theory of multi-point kinetics

The safety assessment of several transients in nuclear reactors requires the simulation of the dynamic behaviour. However, the space independent version of the neutron balance equations, though computationally simple is unacceptable for large core coupled calculations. For this reason, several methods for the solution of the time-dependent neutronic equations have been developed over the years. Development of interconnected models for space and amplitude of neutron flux is the most sophisticated approach in this direction and is known as space-time kinetics analysis. However, computing effort associated with such formulation is very large and therefore some intermediate methods of modest accuracy to address core asymmetry in selected problems are explored. The multi-point kinetics is one such method. It was proposed long back in late 1950s for the kind of reactor dynamics problems in which different parts of a nuclear system evolve with little mutual influence. Under these situations the kinetic equations for each subdomain can be derived in terms of its own amplitude function, properly connected to the others through coupling coefficients. These coefficients were mainly computed through physical considerations. In summary, among the various methods, multi-point kinetics method, from which simple first order equations governing node averaged power can be cast rather easily, form a better candidate under many scenarios. Moreover, with transient simulations being an integral part of the control system design and analysis task, such models further establish their relevance in loss of regulation accident (LORA) and control related applications. Over the period of time, multi-point kinetics models have been used extensively for the analysis and simulation of light water reactors (LWRs) and control system design of PHWRs (Dulla and Picca, 2006).

The detailed derivation of general multi-point kinetics model from multi-group neutron diffusion equations provided by Shimjith et al. (2013) is reproduced here and adapted for two-point formulation. The two group equations and associated delayed neutron precursors concentration equations are as follows

$$\frac{1}{v_1}\frac{\partial \emptyset_1}{\partial t} = \nabla.(D_1\nabla\emptyset_1) - \Sigma_{a1}\emptyset_1 - \Sigma_{12}\emptyset_1 + \Sigma_{21}\emptyset_2 + \left(1-\beta\right)\left(\nu\Sigma_{f1}\emptyset_1 + \nu\Sigma_{f2}\emptyset_2\right) + \sum_{i=1}^{m_d}\lambda_i\tilde{C}_i \quad (1)$$

$$\frac{1}{v_2}\frac{\partial \emptyset_2}{\partial t} = \nabla.(D_2\nabla\emptyset_2) - \Sigma_{a2}\emptyset_2 + \Sigma_{12}\emptyset_1 - \Sigma_{21}\emptyset_2 \quad (2)$$

$$\frac{\partial \tilde{C}_i}{\partial t} = \beta_i\left(\nu\Sigma_{f1}\emptyset_1 + \Sigma_{f2}\emptyset_2\right) - \lambda_i\tilde{C}_i; \quad i = 1, 2, \ldots . m_d \quad (3)$$

where $\emptyset_1$ denotes fast neutron flux, $\emptyset_2$ denotes thermal neutron flux, $\tilde{C}_i$ is the precursor concentration of the ith delayed neutron group and m_d is the number of delayed neutron groups. It is assumed that all the fission neutrons generated are fast neutrons. The fluxes $\emptyset_1$ and $\emptyset_2$ are functions of both space and time. Also the parameters $D_1, D_2, \Sigma_{a1}, \Sigma_{a2}, \Sigma_{f1}, \Sigma_{f2}$ are different at different locations of the core. Now let the core be divided into a number of small mesh boxes called nodes. For each mesh box (node h say) the leakage terms in Eqs. (1) and (2) can be represented by

$$\nabla.(D_1\nabla\emptyset_1) \cong D_1\nabla^2\emptyset_{1h} \quad (4)$$

$$\nabla.(D_2\nabla\emptyset_2) \cong D_2\nabla^2\emptyset_{2h} \quad (5)$$

The net rate of fast neutron flow from h to its neighbour k can be approximated as

$$D_1\nabla^2\emptyset_1 V_h = D_1\left(\frac{\partial^2\emptyset_1}{\partial x^2} + \frac{\partial^2\emptyset_1}{\partial y^2} + \frac{\partial^2\emptyset_1}{\partial z}\right)V_h \quad (6)$$

where V_h is the volume of box h.

In generic form it can be written as

$$D_1\frac{\partial^2\emptyset_1}{\partial r^2}V_h = J_r A_{hk}, \quad r = x, y, \quad or \quad z \quad (7)$$

where A_{hk} is the area of interface between h and k and J_r is the neutron current density. From Fick's law

$$J_r = -D_1\frac{\partial\emptyset_1}{\partial r} = \frac{D_1(-\emptyset_{1h} + \emptyset_{1k})}{\Delta_{hk}} \quad (8)$$

where Δ_{hk} is the centre to centre distant between two boxes.

Hence

$$\nabla.(D_1\nabla\emptyset_1) \cong D_1\nabla^2\emptyset_{1h} = \frac{J_r A_{hk}}{V_h} = \frac{D_1 A_{hk}(-\emptyset_{1h} + \emptyset_{1k})}{V_h\Delta_{hk}} \quad (9)$$

If there are many nodes like k, then

$$D_1\nabla^2\emptyset_{1h} = -\omega_{1hh}\emptyset_{1h} + \sum_{k=1,k\neq h}^{Z}\omega_{1hk}\emptyset_{1k} \quad (10)$$

Similarly for thermal neutron flux

$$D_2\nabla^2\emptyset_{2h} = -\omega_{2hh}\emptyset_{2h} + \sum_{k=1,k\neq h}^{Z}\omega_{2hk}\emptyset_{2k} \quad (11)$$

Where

$$\omega_{ihk} = \frac{D_i A_{hk}}{V_h\Delta_{hk}} \text{ and } \omega_{ihh} = \sum_{k=1,k\neq h}^{Z}\omega_{ihk}, \quad i = 1, 2 \quad (12)$$

The total number of nodes including h is Z. The summation is required for neighbour boxes only as for non-neighbours ω_{ihk} is zero. With this, the group fluxes are function of time only for each mesh box. Hence for mesh box h Eqs. (1) and (2) become

$$\frac{1}{v_{1h}}\frac{d\emptyset_{1h}}{dt} = -\omega_{1hh}\emptyset_{1h} + \sum_{k=1,k\neq h}^{Z}\omega_{1hk}\emptyset_{1k} - \Sigma_{a1h}\emptyset_{1h} - \Sigma_{12h}\emptyset_{1h} + \Sigma_{21h}\emptyset_{2h} + \left(1-\beta\right)\left(\nu\Sigma_{f1h}\emptyset_{1h} + \nu\Sigma_{f2h}\emptyset_{2h}\right) + \sum_{i=1}^{m_d}\lambda_i\tilde{C}_{ih} \quad (13)$$

$$\frac{1}{v_{2h}}\frac{d\emptyset_{2h}}{dt} = -\omega_{2hh}\emptyset_{2h} + \sum_{k=1,k\neq h}^{Z}\omega_{2hk}\emptyset_{2k} - \Sigma_{a2h}\emptyset_{2h} + \Sigma_{12h}\emptyset_{1h} - \Sigma_{21h}\emptyset_{2h} \quad (14)$$

Adding these two Eqs. (13) and (14) and defining flux weighted terms as

$$\omega_{hh} = \frac{\omega_{1hh} + \omega_{2hh}R_h}{1+R_h}, \quad \omega_{hk} = \frac{\omega_{1hk} + \omega_{2hk}R_h}{1+R_h}$$

$$\Sigma_{fh} = \frac{\Sigma_{f1h} + \Sigma_{f2h}R_h}{1+R_h}, \quad \Sigma_{ah} = \frac{\Sigma_{a1h} + \Sigma_{a2h}R_h}{1+R_h}$$

$$\frac{1}{\nu_h} = \frac{\left(1/\nu_{1h}\right) + \left(\left(1/\nu_{2h}\right)R_h\right)}{1+R_h}, \quad \emptyset_h = \emptyset_{1h} + \emptyset_{2h}, \quad R_h = \frac{\emptyset_{2h}}{\emptyset_{1h}}$$

The following one group equation is obtained

$$\frac{1}{\nu_h}\frac{d\emptyset_h}{dt} = -\omega_{hh}\emptyset_h + \sum_{k=1,k\neq h}^{Z}\omega_{hk}\emptyset_k - \Sigma_{ah}\emptyset_h + \left(1-\beta\right)\nu\Sigma_{fh}\emptyset_h + \sum_{i=1}^{m_d}\lambda_i\tilde{C}_{ih} \tag{15}$$

To evaluate the equivalent one group terms, the ratio of fast flux to thermal flux for each mesh box needs to be evaluated. To do that both the fast and thermal neutron balance equations can be solved for each mesh box and R_h can be evaluated. But this would be computationally expensive. To circumvent this as an approximation the steady state form of thermal neutron flux is considered along with the assumption that leakage of thermal neutrons is negligible. Then

$$\begin{aligned} 0 &\approx -\Sigma_{a2h}\emptyset_{2h} + \Sigma_{12h}\emptyset_{1h} - \Sigma_{21h}\emptyset_{2h} \\ \Rightarrow R_h &= \frac{\emptyset_{2h}}{\emptyset_{1h}} \approx \frac{\Sigma_{12h}}{\Sigma_{a2h}+\Sigma_{21h}} \end{aligned} \tag{16}$$

Similarly the delayed neutron precursor concentration equation becomes

$$\frac{d\tilde{C}_{ih}}{dt} = \beta_{ih}\nu\Sigma_{fh}\emptyset_h - \lambda_i\tilde{C}_{ih}; \quad i = 1,2,\ldots.m_d \tag{17}$$

Now transforming the fluxes to powers

$$P_h = E_{\text{eff}}\Sigma_{fh}V_h\emptyset_h$$

Accordingly delayed neutron precursor as

$$C_{ih} = \tilde{C}_{ih}E_{\text{eff}}\Sigma_{fh}V_h\nu_h$$

The equations become

$$\frac{dP_h}{dt} = -\omega_{hh}\nu_h P_h + \sum_{k=1,k\neq h}^{Z}\frac{\omega_{hk}\Sigma_{fh}V_h}{\Sigma_{fk}V_k}\nu_h P_k - \Sigma_{ah}\nu_h P_h + \left(1-\beta\right)\nu\Sigma_{fh}\nu_h P_h + \sum_{i=1}^{m_d}\lambda_i C_{ih} \tag{18}$$

$$\frac{dC_{ih}}{dt} = \beta_{ih}\nu\Sigma_{fh}\nu_h P_h - \lambda_i C_{ih}; \quad i = 1,2,\ldots.m_d \tag{19}$$

Now

$$\omega_{hk} = \frac{\omega_{1hk} + \omega_{2hk}R_h}{1+R_h} = \frac{A_{hk}}{V_h\Delta_{hk}}\left(\frac{D_1 + D_2R_h}{1+R_h}\right) = \frac{D_hA_{hk}}{V_h\Delta_{hk}}$$

Similarly

$$\omega_{kh} = \frac{D_kA_{hk}}{V_k\Delta_{hk}} = \left(\frac{D_1 + D_2R_k}{1+R_k}\right)\frac{A_{hk}}{V_k\Delta_{hk}}$$

Now since R_h and R_k are approximated to ratio of cross sections, they are equal to each other. Hence

$$\omega_{hk}V_h = \omega_{kh}V_k \tag{20}$$

By further defining prompt neutron life time, $l_h = \left(1/\Sigma_{ah}\nu_h\right)$, infinite multiplication factor $K_h = \left(\nu\Sigma_{fh}/\Sigma_{ah}\right)$ and reactivity $\rho_h = \frac{(K_h-1)}{K_h}$ for each mesh box and

$$\alpha_{hh} = \omega_{hh}\nu_h l_h \quad \text{and} \quad \alpha_{kh} = \frac{\omega_{hk}\Sigma_{fh}V_h\nu_h l_h}{\Sigma_{fk}V_k} \tag{21}$$

The equations become

$$\frac{dP_h}{dt} = -\alpha_{hh}\frac{P_h}{l_h} + \sum_{k=1,k\neq h}^{Z}\alpha_{kh}\frac{P_k}{l_h} + \left(\rho_h - \beta\right)\frac{P_h}{l_h} + \sum_{i=1}^{m_d}\lambda_i C_{ih} \tag{22}$$

$$\frac{dC_{ih}}{dt} = \beta_{ih}\frac{P_h}{l_h} - \lambda_i C_{ih}; \quad i = 1,2,\ldots.m_d \tag{23}$$

For the simplifying case of reactor core being represented by two mesh boxes (nodes) the equations become

$$\frac{dP_h}{dt} = -\alpha_{hh}\frac{P_h}{l_h} + \alpha_{kh}\frac{P_k}{l_h} + \left(\rho_h - \beta_h\right)\frac{P_h}{l_h} + \sum_{i=1}^{m_d}\lambda_i C_{ih} \tag{24}$$

$$\frac{dC_{ih}}{dt} = \beta_{ih}\frac{P_h}{l_h} - \lambda_i C_{ih}; \quad i = 1,2,\ldots.m_d \tag{25}$$

$$\frac{dP_k}{dt} = -\alpha_{kk}\frac{P_k}{l_k} + \alpha_{hk}\frac{P_h}{l_k} + \left(\rho_k - \beta_k\right)\frac{P_k}{l_k} + \sum_{i=1}^{m_d}\lambda_i C_{ik} \tag{26}$$

$$\frac{dC_{ik}}{dt} = \beta_{ik}\frac{P_k}{l_k} - \lambda_i C_{ik}; \quad i = 1,2,\ldots.m_d \tag{27}$$

4. Salient aspects of system modelling

In primary heat transport (PHT) system of the PHWR under consideration, there are two figure-of-eight loops. Each loop has two passes (forward flow and reverse flow) consisting of a number of parallel channels. The schematic of the PHT system for one loop is shown in Fig. 2.

The nodalisation of primary and secondary system is shown in Fig. 3. In each PHT system loop, two RIHs and two ROHs have been modelled as branch components. The loop containing the broken header (RIH-1) is the broken loop and the other loop is the intact loop. In broken loop, the channels connecting broken

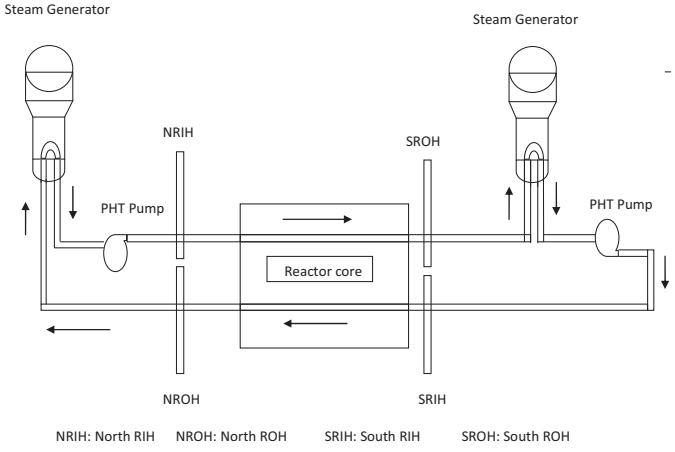

Fig. 2. Schematic of primary heat transport system (showing one loop).

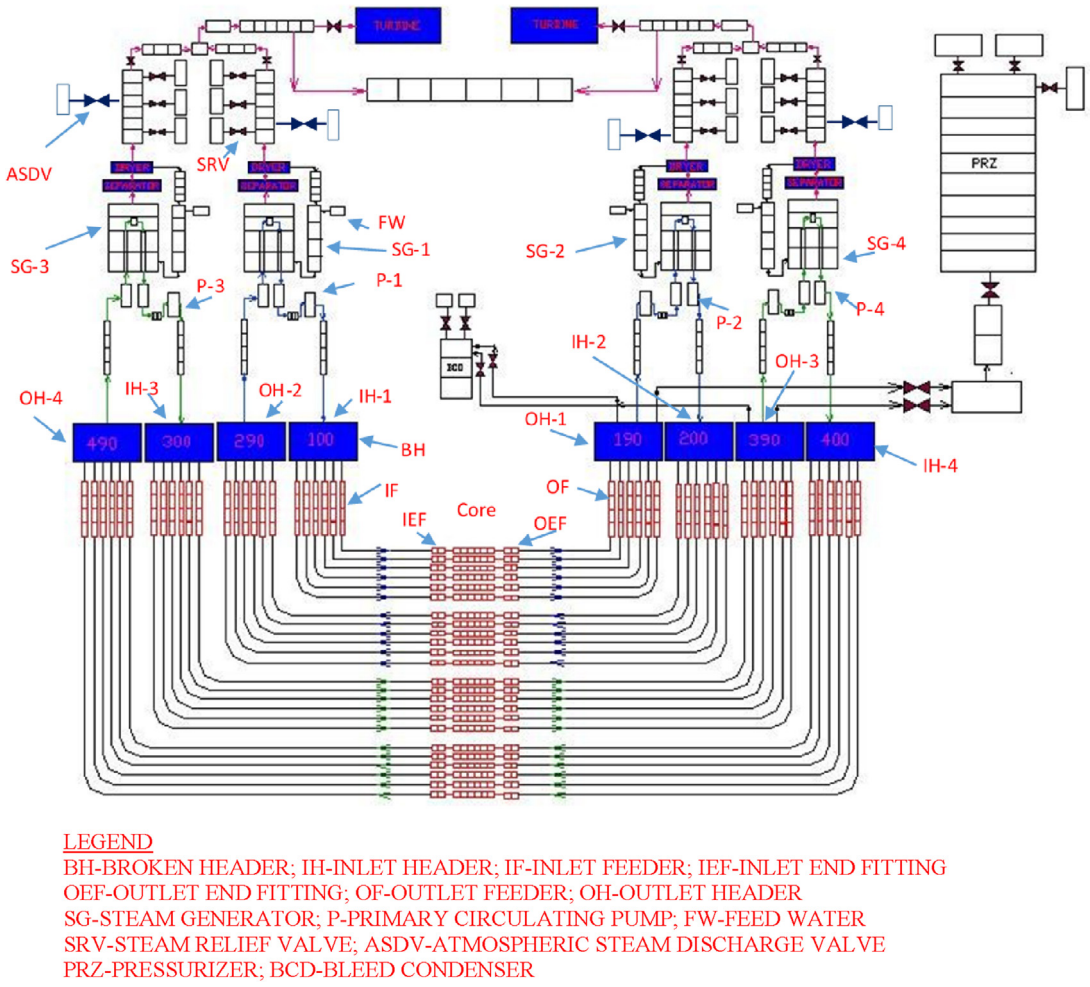

Fig. 3. Nodalization of primary and secondary system.

header (RIH-1) and ROH-1 is called broken pass and the channels connecting RIH-2 to ROH-2 is called unbroken pass. All coolant channels of each pass are clubbed into nine pipe components (for clarity in Fig. 3. only six are shown) and corresponding heat structures. Each pipe component is divided in eight control volumes ((for clarity in Fig. 3. only six are shown). Appropriate axial and radial power profiles for fuel bundles (modelled as heat structures) were provided in the input. Out of all of the forward flow or reverse flow coolant channels, one maximum powered channel was considered and the remaining channels were clubbed in eight average powered channels. Inlet and outlet feeders and inlet and outlet end fittings were modelled as pipe component with four and two control volumes respectively. Equivalent pipe diameter and length along with loss coefficients are considered for modelling the end-fitting. The feeder is connected with end-fitting by single junction having appropriate loss coefficient. Pump suction and discharge lines were modelled as pipe component.

Fuel rod was modelled as heat structure with eight radial mesh points and eight axial nodes (each corresponding to one node of channel). The fuel pellet, pellet-clad gap and clad were divided into three, one and four radial intervals respectively. Heat transfer from fuel rod to primary coolant is modelled with inbuilt model of RELAP5 for horizontal rod bundles.

Primary Circulating Pump (PCP) was modelled with inbuilt model for Westinghouse pump in RELAP5/MOD3.4 and the corresponding inbuilt homologues data was used. Coast down curve for the pump was provided with speed of the pump versus time after trip of PCP. Pressurizer with heater, surge line and relief valve was also modelled. The pressurizer is connected to the south side outlet header of the two loops. Instrumented relief valve (IRV) pipe line is connected to SROH (South Reactor Outlet Header) of two loops and IRV discharge is connected to bleed condenser. ECCS accumulator, surge line, related valves and pipe connecting inlet and outlet headers were modelled. ECCS recirculation line was modelled with time dependent volume (TDV) with the mass flow rate as boundary condition based on primary pressure.

In secondary system, main feed water and auxiliary feed water supply systems were modelled using several volumes and junctions. Containment is modelled as a constant pressure volume with atmospheric condition. A trip valve is connected to containment at the exit face of reactor inlet header. The trip valve simulates the break in inlet header. The flow area of break valve is a measure of the percentage (%) of break.

Initially in-built point reactor kinetics model of RELAP5 was considered in the reactor core and later calculations were carried out using the verified and validated multi-point kinetics model. Axial peaking factor is provided in the input deck according to reactor physics data. The total power of the reactor is normalized to one. Feedback effects of coolant void and fuel temperature were considered. Reactivity SCRAM table was provided for shutting down the

reactor. Decay heat after reactor shut down is also considered in the modelling.

4.1. Modeling assumptions

In this analysis, following assumptions have been considered:

(i) Credit of feed and bleed system is not taken in the analysis.
(ii) Reactor Regulation System is not modelled.
(iii) For tripping the reactor, equivalent SCRAM table is provided.
(iv) Effective fraction of delayed neutrons and prompt neutrons life time are assumed maximum, so that the rate of reactor power decrease during the reactor SCRAM is minimum.
(v) Coolant void coefficient of reactivity and fuel temperature coefficient of reactivity are assumed conservatively in the analysis.
(vi) One Atmospheric Steam Dump Valve (ASDV) is assumed to be failed and one Safety Relief Valve (SRV) of each steam generator (SG) is also assumed to be failed.
(vii) The crash cool down is initiated after 2 s of the start of the transient.

4.2. Initial and boundary conditions

Steady state is achieved after a code run of 2000 s with both in-built and user defined multi-point kinetics model. The secondary side feed water flow is maintained constant at a value corresponding to main feed water flow with a time dependent junction. After reactor trip, it decreases to a value corresponding to auxiliary feed water flow and remains constant. The PCP coasts down as per the time dependent velocity curve provided in the input file. The steady state value of important parameters as obtained in the simulation is provided in Table 1 along with the design value. The same steady state is obtained with in-built and user defined multi-point kinetics model.

5. Event sequence

Transient is initiated with a break in the RIH of one loop. To find out the critical break size, different cases are analyzed having break sizes ranging from 5% to 100% of double ended RIH break.

The postulated scenario is as follows:

(i) Transient is initiated at $t = 2000$ s of steady state run with initiation of different break sizes in the RIH.
(ii) Reactor trip signal is generated on low RIH pressure or high reactor power or high rate log power depending on break sizes.
(iii) PCPs, turbine and main feed water pump trip on reactor trip.
(iv) Pressurizer is isolated on low PHT pressure.
(v) ECCS actuation on low PHT pressure.

The event sequence and phenomena depend on the break size. The general pattern is described here. Following the pipe break, the coolant starts discharging out of the broken location and attains the critical flow conditions. In the initial period, reactor being in sub cooled condition depressurizes very fast, and subsequently the discharge rate falls after attaining the maximum due to sharp reduction in the upstream pressure. The discharge rate decreases further due to formation of more voids.

The core flow decreases in broken pass and increases (initially) in unbroken pass. The initial increase in flow in unbroken pass is mainly due to increase in differential pressure in this pass, which is a result of higher pressure reduction in ROH of that pass compared to corresponding RIH. As the pressure decreases in the broken node very fast, flow reversal may occur in the broken pass. Due to non-operation of PCPs, core flow reduces in intact loop. At the reduced core flow, differential temperature rise across core is large, resulting in higher coolant temperature at ROH and higher void fraction.

Table 1
Steady state values of important system parameters.

Sr. no.	Parameters	Design nominal value	Location	Steady state value
1	ROH pressure (MPa)	9.908 (100 kg/cm^2 (g))	ROH-1	9.8954
			ROH-2	9.8759
			ROH-3	9.8952
			ROH-4	9.8759
2	RIH pressure (MPa)	11.448 (115.89 kg/cm^2 (g))	RIH-1	11.4693
			RIH-2	11.4886
			RIH-3	11.4688
			RIH-4	11.4880
3	RIH temp. (K)	533.15 (260 °C)	RIH-1	534.13
			RIH-2	534.17
			RIH-3	534.32
			RIH-4	534.36
4	ROH temp. (K)	577.15 (304 °C)	ROH-1	576.93
			ROH-2	576.95
			ROH-3	577.19
			ROH-4	577.21
5	Flow rate per pass (pump discharge flow) (kg/s)	1947.1	PCP-1	1960.1
			PCP-2	1960.1
			PCP-3	1959.2
			PCP-4	1959.3
6	SG pressure (MPa)	4.1711 (41.5 kg/cm^2 (g))	SG-1	4.1768
			SG-2	4.1904
			SG-3	4.1805
			SG-4	4.1925

6. Development of multi-point kinetics model

The in-built point kinetics model of RELAP5 was put off and user defined single and multi-point kinetics models were introduced. The complete model was developed in a phase wise manner. The results were compared with that of in-built point kinetics model of RELAP5 and also validated against in-house developed 3D kinetics code TRIKIN (Obaidurrahman et al., 2010; Jain and Obaidurrahman, 2012). The transient analysed is 22.5% break in one RIH of one loop with class-IV power supply unavailable. For all the different cases analyzed, steady state is obtained after a code run of 2000 s.

6.1. Development of user-defined kinetics model

In the first step towards development of user-defined kinetics model for incorporation in RELAP5, the reactor was modelled as one point. Decay heat was not modelled for first case but subsequently it was considered. In using RELAP5 default kinetics model, always six groups of delayed neutrons are considered. Both one group and six groups of delayed neutrons are modelled in user-defined point kinetics model. The neutron balance equation along with concentration of delayed neutron pre-cursor was solved using Euler's method for every time step (McMahon and Pierson, 2010; Abdallah, 2011). The calculated power was fed into the fuel bundles modelled as heat structures. The results are shown in Fig. 4.

It is observed that, there is significant difference between one group and six-group delayed neutron modelling with respect to rate of power rise and the maximum reactor power. As can be seen from the figure, the user defined kinetics model with six group delayed neutron matches closely with that of RELAP5 in-built model both in trend and magnitude. Hence it was decided, to go forward with six groups of delayed neutrons.

6.2. Development of user-defined multi-point kinetics model

In the next step, two-core (multi-point) model was developed in which the reactor was modelled as two regions each representing one loop. It was assumed that each core was at critical state. The results are shown in Fig. 5. As expected, the power of core representing broken loop rises significantly since the void effect is localized to that loop. There is very less increase in the power of core representing intact loop. The average power shown is the power of the reactor comprising both broken loop and intact loop. It is not possible to get different powers for different loops in default kinetics model of RELAP5.

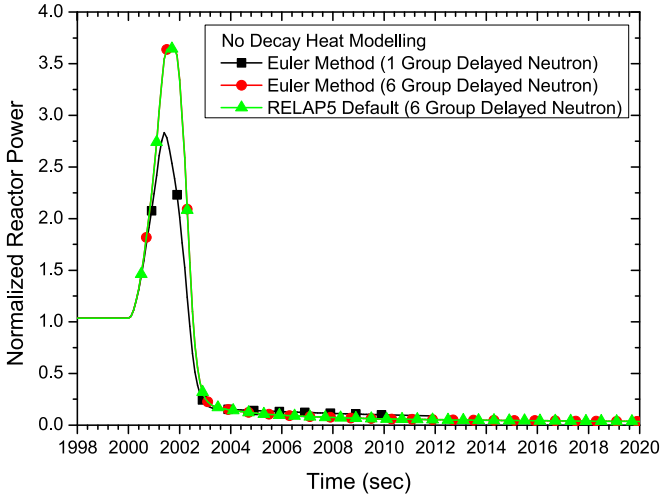

Fig. 4. Single point kinetics with different delayed neutron groups.

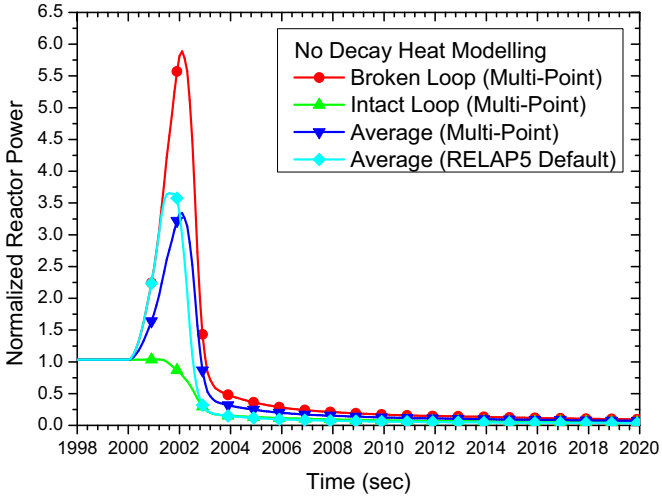

Fig. 5. Multi-point kinetics with six delayed neutron groups.

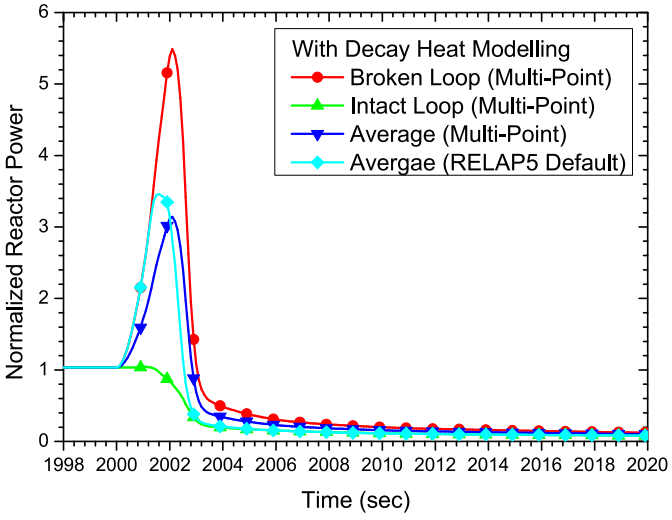

Fig. 6. Multi-point kinetics with standard decay heat model.

6.3. Development of user-defined decay heat model

Standard decay heat model of Way & Wigner was considered.

Way & Wigner Model (standard formula) (Todreas and Kazimi, 1990; Glasstone and Sesonske, 1981):

$$\frac{P}{P_0} = 0.066\left(T_s^{-0.2} - T^{-0.2}\right) \tag{28}$$

where P = decay power at time T ($=T_0+T_s$), P_0 = steady reactor power, T_s = time after shutdown, T_0 = time for which reactor was at steady power P_0.

The results are shown in Fig. 6. The rise of power in broken loop is very high. In reality, the rise will be less since there is diffusion of neutrons from high flux zone to low flux zone. To realistically estimate the power of broken and intact loop, leakage of neutrons from broken to intact and vice-versa are modelled as described in next section.

6.4. Development of user-defined multi-point kinetics with decay heat and diffusion model

To account for the diffusion of neutrons from one core to other, additional terms are incorporated into the neutron balance equation through use of coupling coefficients. The coupling coefficients

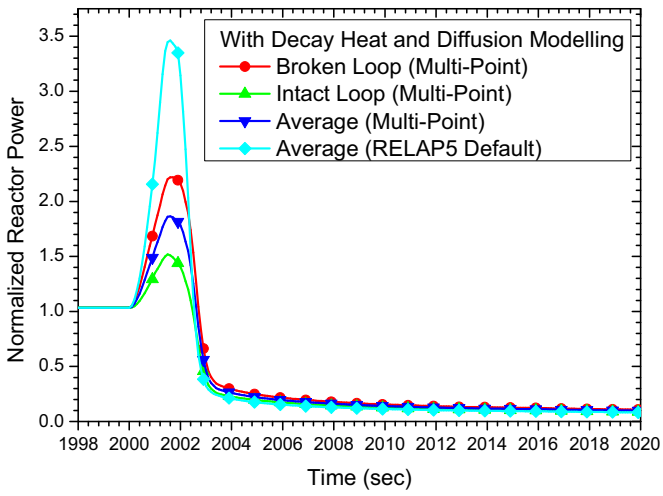

Fig. 7. Multi-point kinetics with standard decay heat model and diffusion.

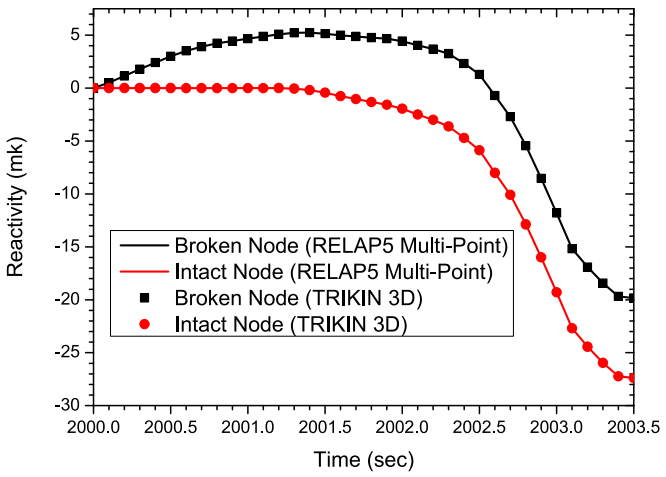

Fig. 9. Nodal reactivity in RELAP5 and TRIKIN.

$(\alpha_{kh}, \alpha_{hk})$ are estimated using formula described in Section 3. The value of α_{kh} was found to be 5.1608E − 3. Identical steady state flux level, material and dimensions of both nodes, broken as well as intact node lead to similar magnitude of coupling coefficients α_{kh} and α_{hk}. The results are shown in Fig. 7. As expected the power rise in broken loop decreased and intact loop increased compared to that of the case where neutron leakage from one core to the other is not modelled. Surprisingly the rise in power of broken loop is lesser than that of RELAP5 default model (single region). This is attributed to the fact that in RELAP5 in-built model, decay dynamics is modelled where the decay power rises when there is rise in fission power. But in the user defined model the decay power is assumed constant till the reactor is shutdown. The decay dynamics model will be developed in a later stage.

7. Validation of multi-point kinetics model

The core configuration of AECL three dimensional kinetics benchmark problem in a heavy water reactor (Judd and Rouben, 1981) was considered for validation. The PHWR with this core configuration was modelled using both multi-point kinetics model and in-house 3-D kinetics code TRIKIN. Except reactor physics parameters, other aspects of RELAP5 modelling remains the same as described in previous sections. The core geometry is shown in Fig. 8.

Only the inner and outer core region was modelled excluding the reflector region (regions marked 1,2,3 4).

TRIKIN is an in-house developed kinetics code based on a flux factorization technique employed by the improved quasi-static (IQS) method. The core physics calculations are based on the finite differencing scheme of the TRIHEX-FA code (Jagannathan, 2006). The code is validated against a series of bench mark exercises (Obaidurrahman et al., 2010; Jain and Obaidurrahman, 2012). Six number of delayed neutron groups and two group neutron energy was modelled in TRIKIN. The total number of cells in x, y and z direction are, respectively 18, 18 and 10.

The coupling coefficients $(\alpha_{kh}, \alpha_{hk})$ for multi-point kinetics model were estimated using formula described in Section 3. The value of α_{kh} was found to be 5.8444E − 3. The individual node reactivity as a function of time obtained from RELAP5 was superimposed in TRIKIN by artificially changing the removal cross section of each cell (Fig. 9). In TRIKIN, the node reactivity is defined as follows

$$\rho_h = \frac{\sum_{i=1}^{N_h} \left(\nu\Sigma_{f1}\emptyset_1 + \nu\Sigma_{f2}\emptyset_2\right)_i V_i}{\sum_{i=1}^{N_h} (\Sigma_{a1}\emptyset_1 + \Sigma_{a2}\emptyset_2)_i V_i} \quad (29)$$

N_h = number of cells for node h

$$\rho_k = \frac{\sum_{i=1}^{N_k} \left(\nu\Sigma_{f1}\emptyset_1 + \nu\Sigma_{f2}\emptyset_2\right)_i V_i}{\sum_{i=1}^{N_k} (\Sigma_{a1}\emptyset_1 + \Sigma_{a2}\emptyset_2)_i V_i} \quad (30)$$

N_k = number of cells for node k

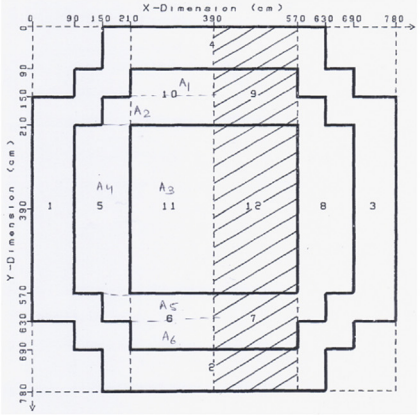

Material Region	Description
Inner Core and Outer Core	fuel: natural UO_2 at 600°C coolant: 99.7% D_2O at 270°C moderator: 99.7% D_2O at 60°C
Reflector	99.7% D_2O at 60°C

Boundary Conditions:

External: zero flux

Fig. 8. Vertical cross section at $Z = 0$ cm (total depth 600 cm).

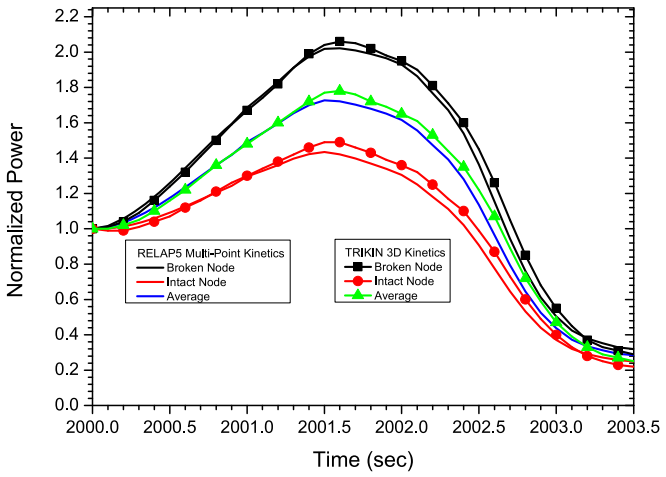

Fig. 10. Normalized power in RELAP5 and TRIKIN.

In the present calculation $N_h = N_k$. The normalized power for each node (loop) obtained from RELAP5 and TRIKIN is presented in Fig. 10. The trends of normalized power from RELAP5 as well as TRIKIN matched each other. There is close agreement in the node power prdecticted by RELAP5 and TRIKIN. For node *h*, the maximum value of power from RELAP5 is 2.0218 as compared to TRIKIN of 2.06. while for node *k*, the maximum value of power from RELAP5 is 1.4349 as compared to TRIKIN of 1.49. The minor variations can be attributed to difference in modelling approach in TRIKIN as compared to that of RELAP5. Also the coupling coefficients are static as these are approximated on the basis of steady state parameters. In reality, as the transient progresses, due to change in neutronic parameters these coefficients should change.

8. Results and discussion

The user-defined multi-point kinetics model developed in RELAP5 (Section 6.4) was used to identify the critical break in RIH with class-IV power supply unavailable in a typical large PHWR. For a particular range of break in RIH, gross flow stagnation may occur in the reactor core leading to rise in fuel temperature. The size of the break that leads to maximum rise in clad surface temperature is called critical break. The critical breaks impose most severe requirement on ECCS. A range of break sizes ranging from 5% to 100% of double ended guillotine rupture of RIH are analysed. The transients are analysed up to 50 s after break is initiated since the rise in temperature is maximum in this period. As the reactor is shut down, the decay power is less and at a later stage ECCS water will get injected leading to enhanced core cooling and decrease in temperature of fuel.

8.1. Reactor power

The variation of normalized reactor power in broken loop (node *h*) for different break sizes with respect to time is shown in Fig. 11. Following a break, due to loss of coolant voids are generated in the core. Due to positive void coefficient of reactivity, the reactor power rises sharply. The reactor trips on low header pressure or high reactor power or high rate log power. Since the rate of power rise is high, the reactor power continues to rise even after reactor trip for some time before attaining a maximum value. As expected, the power rise is highest for double ended break since the loss of coolant is highest. The reactor continues to operate with decay power level. The peak value of power is different for different break sizes and as can be seen from the figure it increases with break size.

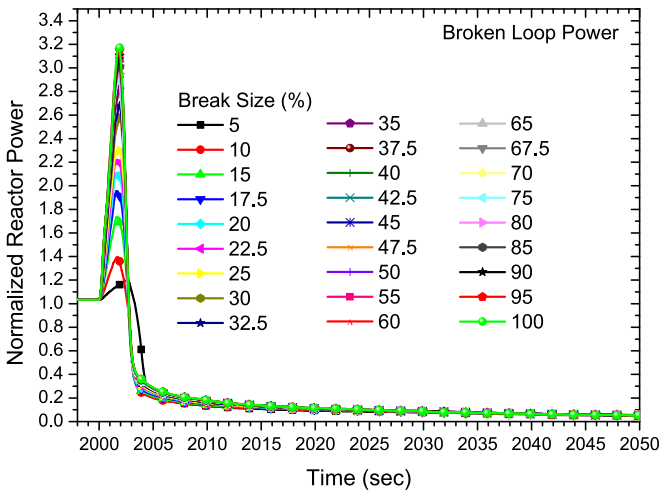

Fig. 11. Normalized reactor power.

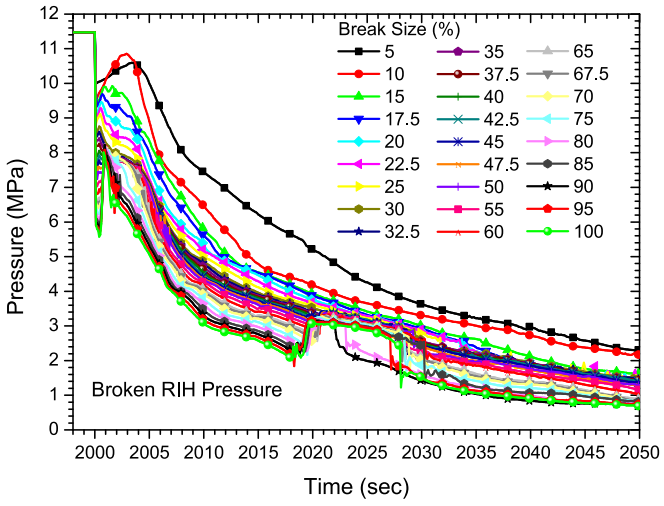

Fig. 12. Reactor inlet header pressure.

8.2. System pressure

The time evolution of system pressure for broken RIH for different break sizes is shown in Fig. 12. Due to loss of coolant, the pressure decreases suddenly. Since the reactor power increases, the pressure increases for some time and then decreases due to both loss of coolant and decrease in reactor power. At any instant, the header pressure is high for lower break sizes. This is due lesser loss of inventory. For higher break sizes, the rate of decrease in pressure decreases at around 10 s after the accident due to ECCS actuation. At around 20 s after the accident (for break sizes greater than 75%), the reactor pressure rises due to mismatch in the rate of loss of coolant and rate of ECCS injection. Once the voids get quenched, the break flow increases due to higher discharge of coolant in liquid phase leading to decrease in header pressure again.

8.3. Mass flow

The mass flow rate of coolant in hot channel of affected pass in the broken loop is shown in Fig. 13. Immediately after break, the flow is reduced due to loss of coolant and loss of forced circulation. For higher break sizes, there occurs flow reversal in the core. The flow in the channel reduces to very low value and except for very low (less than 10%) or high break sizes (more than 50%), the coolant is nearly stagnant. The rate of decrease in flow in the channel for

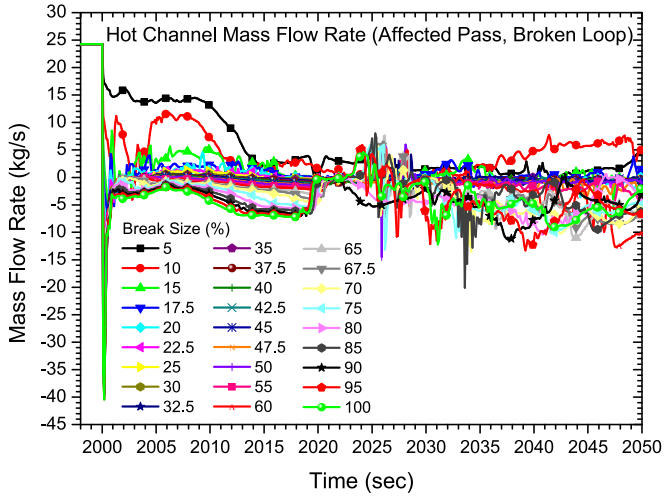

Fig. 13. Core mass flow rate in hot channel (affected pass).

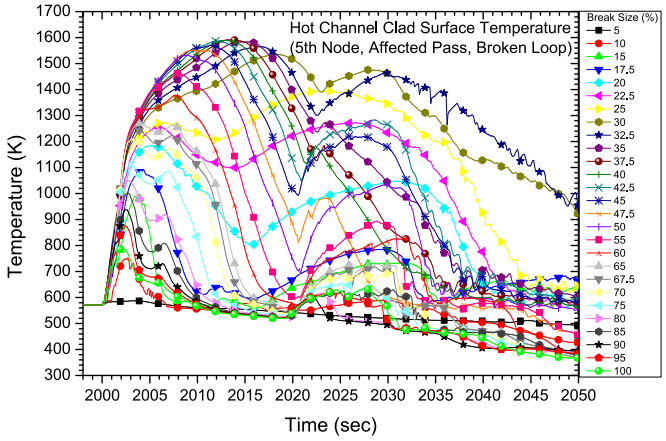

Fig. 14. Clad surface temperature of hot channel (affected pass).

higher break sizes decreases at around 15 s after the accident due to injection of coolant from accumulator. For higher break sizes (greater than 75%), at around 20 s, the magnitude of flow in the core decrease (i.e., moves towards stagnant) due to mismatch in ECCS flow and break flow. With ECCS flow becoming higher than break flow, forward flow occurs in the channel.

8.4. Fuel temperature

The clad surface temperature of central node (5th) in hot channel of broken pass (affected pass) in broken loop is shown in Fig. 14 for different break sizes. The general trend is that the clad surface temperature rises immediately after break due to loss of coolant and rise in reactor power. After attaining a maximum value it decreases and after some time it rises again before decreasing. The rise in temperature is highest in middle range breaks due to flow stagnation in the channel.

9. Identification of critical break

A post-processor code using GNU Fortran was developed to find out the location and magnitude of peak clad surface temperature and maximum fuel centreline temperature for each break size analysed. As the break size increases, the peak clad temperature (PCT) also increases. It reaches a maximum value of 1605.85 K for break

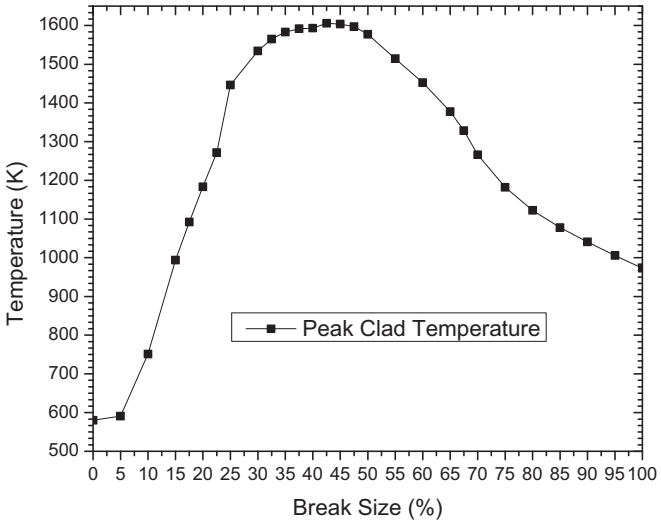

Fig. 15. Peak clad temperature.

size of 42.5% and thereafter it decreases. This is the critical break size. The maximum centreline temperature is highest for break size of 55%. The variation of PCT and with break sizes is shown in Fig. 15. Also shown in the figure is the PCT for 0% break i.e. PCT for nominal case at steady state.

10. Conclusion

Development and implementation of multi-point kinetics model for RELAP5 code through internal coupling using Euler's formulation rendered an important feature to analyse asymmetric core nuclear transients in large loosely coupled power reactors. Initial verification of the model was carried out by comparison of single point kinetics model using this formulation with RELAP5 kinetics results and has shown good agreement. Single point formulation does not bring out difference between intact and broken loops power and consequent core safety parameters for safety assessment. This limitation was addressed in multipoint formulation where the estimated power rise in the intact (unbroken) loop was very less. The coupling coefficients were estimated from steady state neutronics parameters and were assumed constant throughout the transient. The model was validated against 3D kinetics code TRIKIN through numerical tuning of local removal cross section of each cell to conserve the nodal reactivity obtained from RELAP5. Observed minor deviations of about 2% in normalized power between multipoint and 3D formulation can be attributed to limitations of present multipoint formulation in regard to number of nodes, limited energy groups and fixing of multipoint coupling coefficient in time domain during evolving nuclear transient. This can be improved through time updating of inter node coupling coefficients based on instantaneous thermal state of respective node. This has been planned in the next stage of development. The developed model has been successfully used to identify critical break in RIH with class-IV power supply unavailable in a large sized PHWR core.

References

Abdallah, A. Nahla, 2011. Taylor's series method for solving the nonlinear point kinetics equations. Nucl. Eng. Des. 241 (2011), 1592–1595.

Dulla, S., Picca, P., 2006. Consistent multipoint kinetics for source-driven systems. Prog. Nucl. Energy 48, 617–628.

Espinosa-Paredes, G., Nunez-Carrera, A., 2008. SBWR Model for Steady-State and Transient Analysis, Science and Technology of Nuclear Installations. Hindawi Publishing Corporation (Article ID 428168).

Glasstone, S., Sesonske, A., 1981. Nuclear Reactor Engineering. Krieger Publishing Company, ISBN 0-89464-567-6 (3rd edition).

Information Systems Laboratories Inc, 2001. RELAP5/MOD 3.3 Code Manual, NUREG/CR-5535 Rev 1—Volume I-VIII.

Jagannathan, V., et al., 2006. Validation of finite difference core diffusion calculation methods with FEM and NEM for VVER-1000 MWe reactor. In: PHYSOR-2006, ANS Topical Meeting on Reactor Physics, Vancouver, Canada, Se 10-14.

Jain, R.P., Obaidurrahman, K., 2012. Validation of 3D Kinetics Code 'TRIKIN' using OECD PWR core transient benchmark. Int. J. Nucl. Energy Sci. Technol. 7 (2), 131–142.

Judd, R.A., Rouben, B., 1981. Three dimensional kinetics benchmark problem in a heavy water reactor. In: AECL-7236. Atomic Energy of Canada Limited.

McMahon, D., Pierson, A., 2010. 'A Taylor series solution of the reactor point kinetics equations', arXiv:1001.4100v2[physics.comp-ph], arxiv.org, Cornell University Library ⟨http://arxiv.org/ftp/arxiv/papers/1001/1001.4100.pdf⟩.

Obaidurrahman, K., Singh, O.P., 2010. Spatial neutronic coupling aspects in nuclear reactors. Nucl. Eng. Des. 240, 2755–2760.

Obaidurrahman, K., Doshi, J.B., Jain, R.P., Jagannathan, V., 2010. Development and validation of coupled dynamics code 'TRIKIN' for VVER reactors. Nucl. Eng. Technol. 42 (3), 259–270.

Pradhan, S.K., Prem, P., Gupta, S.K., 2012. 'Methodology for estimation of conditional probability of stagnation channel break for PHWRs', Annals of Nuclear Energy, Vol. 43 pp. 49–55.

Shimjith, S.R., Tiwari, A.P., Naskar, M., Bandyopadhyay, B., 2010. Space-time kinetics modeling of advanced heavy water reactor for control studies. Ann. Nucl. Energy 37, 310–324.

Shimjith, S.R., Tiwari, A.P., Bandyopadhyay, B., 2013. Chapter 2, 'Multipoint Kinetics Modeling of Large Nuclear Reactors' in 'Modeling and Control of a Large Nuclear Reactor', LNCIS, vol. 431. Springer-Verlag, Berlin Heidelberg, pp. 17–60.

Todreas, Neil E., Kazimi, Mujid S., 1990. Nuclear Systems I, Thermal Hydraulic Fundamentals. Taylor and Francis, ISBN 1-56032-051-6 (v. 1).

Zhang, Hongbin, Zou, Ling, Andrs, David, Zhao, Haihua, Martineau, Richard, 2013. Point kinetics calculations with fully coupled thermal fluids reactivity feedback. In: International Conference on Mathematics and Computational Methods Applied to Nuclear Science and Engineering, ISBN 978-1-62748-643-9.